Journal of the Brazilian Society of Mechanical Sciences and Engineering (2020) 42:45
https://doi.org/10.1007/s40430-019-2130-z

TECHNICAL PAPER

Investigation of mechanical and tribological properties of hybrid green eggshells and graphite-reinforced aluminum composites

Mohammed A. Almomani[1] · **Mohammed T. Hayajneh**[1] · **Mu'ayyad M. Al-Shrida**[1]

Received: 11 July 2019 / Accepted: 3 December 2019 / Published online: 14 December 2019

Abstract

Low cost, low density and good thermal stability of hens' eggshells make them a new reinforcement material. Further, eggshell (Es) is considered as a renewable eco-friendly material. Besides, its waste causes insect infestation and therefore pollution problems. Graphite (Gr) is one of the most commonly used reinforcements due to its self-lubricating properties. Hence, the current work aims to use the powder metallurgy technique to fabricate various aluminum matrix composites having different weight percentages of hybrid green particles (eggshells and graphite). Sintering additives such as magnesium and tin were used to improve the density. Firstly, the powders were manually mixed and cold compacted at 475 MPa and then sintered at 630 °C for 2 h. A pin-on-disk wear, Vickers hardness and compressive strength tests were used to investigate the mechanical and tribological properties. Scanning electron microscope (SEM) was used to characterize the morphology and microstructure of the produced composites as well as wear mechanisms. Energy-dispersive X-ray spectroscopy (EDX) test was used to investigate the elemental composition of the composites. The results showed that adding graphite to the aluminum matrix composite containing eggshell has a positive impact on the tribological properties of the composite up to a certain limit (1.5 wt%). However, the additional increase in graphite content has an adverse effect. Hybrid composites with 3 wt% eggshell show the best compressive strength and hardness, whereas hybrid composite with 9 wt% eggshell has the lowest compressive strength and hardness. The mass loss of the hybrid composite increases with the increase in the graphite weight percentages regardless of the eggshell weight percentages. The combination of SEM micrographs and EDX showed signs for three wear mechanisms: abrasive, adhesive and delaminated wear in the examined composites.

Keywords Aluminum matrix composite · Eggshells · Graphite · Hybrid green composites · Powder metallurgy · Pin-on-disk wear test · Micro-Vickers hardness · Compressive strength

1 Introduction

Low hardness and poor tribological properties represent major limitations of aluminum and its alloys [1]. Despite these limitations, aluminum is characterized by its low density, high thermal conductivity and high toughness. Also, it has high corrosion resistance which extends its uses to a wide variety of environmental conditions [2].

Attempts were made to expend the use of aluminum and its alloys by overcoming drawbacks that restrict its use by incorporating various ceramic hard phases such as SiC [3], eggshells (Es) [4], Al_2O_3 [5] and BN [6]. Further, hybrid reinforcements, e.g., fly ash–alumina [7], MoS_2-WC [8], SiC-Es [9], were used to improve mechanical and tribological properties of aluminum alloys.

Eggshell is a ceramic material with low density, low cost and high thermal stability. Further, it is considered as an eco-friendly renewable material [10–14]. Moreover, the good corrosion resistance of graphite encourages the researchers to use as a reinforcement material in aluminum matrix composite, especially that graphite is considered as a good solid lubricant because of the weak Van der Waals bond

Technical Editor: Paulo de Tarso Rocha de Mendonça, Ph.D.

✉ Mohammed A. Almomani
maalmomani7@just.edu.jo

Mohammed T. Hayajneh
hayajneh@just.edu.jo

Mu'ayyad M. Al-Shrida
mmalshrida15@eng.just.edu.jo

[1] Industrial Engineering Department, Faculty of Engineering, Jordan University of Science and Technology, P.O. Box 3030, Irbid 22110, Jordan

between layers of graphite and a strong interlayer covalent bond between carbon atoms [15, 16].

Dispersion of discontinuous reinforcement in the metal matrix is carried out by stir casting or powder metallurgy (PM) technique. In stir casting, the distribution of reinforcement throughout the matrix results in less homogenous products as compared to powder metallurgy in which a highly uniform distribution of reinforcement in the matrix can be attained [17, 18].

The positive effect of graphite (up to a certain limit) on wear resistance was presented in many studies [19–22]. On the other hand, several studies reported that eggshells can improve mechanical properties [9, 23, 24].

To our knowledge, nobody had studied the effect of hybrid green reinforcement (Es–Gr) on the mechanical and tribological properties of the aluminum matrix. Therefore, the current research suggests the use of two kinds of reinforcement, eggshells and graphite, to combine their advantages in one filler material that may overcome the limitations of the aluminum matrix.

2 Experimental details

2.1 Characterization of raw and mixture powders

In this research, composites of aluminum alloy matrix reinforced with two kinds of reinforcements, eggshell and graphite, are prepared by powder metallurgy route. The matrix material was aluminum with a fixed amount of tin (Sn) and magnesium (Mg). The size, shape and density of the materials used in the composites have important effects on the mechanical, tribological and thermal properties of the produced composites [25]. Firstly, powder of commercially pure aluminum of 99% purity provided by Acros Organics, USA, having a density of 2.7 g/cm^3 and particle size of about 74 μm was mixed with a fixed amount of Sn and Mg to form the matrix alloy of the developed composites.

The compressibility of aluminum powders is restricted by the presence of alumina (Al_2O_3) layer surrounding aluminum particles, which prevents particle to particle contact during sintering. Thus, magnesium was used as a sintering agent to react with Al_2O_3 and form crystalline spinel ($3MgAl_2O_4$) and/or (3MgO) which can be easily bonded [26, 27]. Moreover, tin was also used as a sintering agent because of its low melting temperature which prompts phase sintering, leading to denser compact material [28]. Mg and Sn were used with similar and fixed amounts to that used by Macaskill et al. [27]. Accordingly, the matrix alloy composition is Al–1.5Sn–1.5 Mg, and the designation Al matrix will be used to refer to this composition everywhere in this article for simplicity.

Eggshells (Es) powder was used as primary reinforcement material and prepared by collecting raw eggshells from the nearby bakery, cleaning them by water, followed by drying in the sun to remove impurities and unpleasant odors. Plastic hammer was used to convert large shells into flakes that were pulverized by a blender. Next, the carbonization process was performed at 500 °C for 3 h to remove organic materials. During the sintering process, organic materials vaporized and burned off. Figure 1a–c shows raw, carbonized and uncarbonized eggshells, respectively. Finally, the sieving process was carried out by Retsch sieve shaker and the particle size of eggshells was less than 50 μm.

Figure 2a shows SEM images for aluminum particles having elongated sub-angular shape. SEM image shown in Fig. 2b displays the used carbonized eggshell particles having irregular sizes and shapes because of the shear action of the blender blade during preparation. Graphite particles have flake-like shape shown in Fig. 2c. The densities of the reinforcements were determined by Archimedes rule as 2.5 g/cm^3 and 2.1 g/cm^3, for the carbonized eggshell and flakes graphite, respectively. Seven trials were conducted to get more accurate results. Energy-dispersive X-ray spectroscopy (EDX) test was conducted on the eggshells particles to investigate the elemental composition of the composites.

2.2 Densification of mixture powders and processing of hybrid composites

The mixed homogenous powders were compacted at room temperature in a single-action hardened steel die (Φ 8 mm × 20 mm) using a universal testing machine (Fig. 3) (model WAW-2000H) at 475 MPa as concluded from the densification curve shown in Fig. 4 which represents the relationship between the relative density and

Fig. 1 Eggshell samples: **a** uncarbonized (unground); **b** uncarbonized (ground); **c** carbonized (ground)

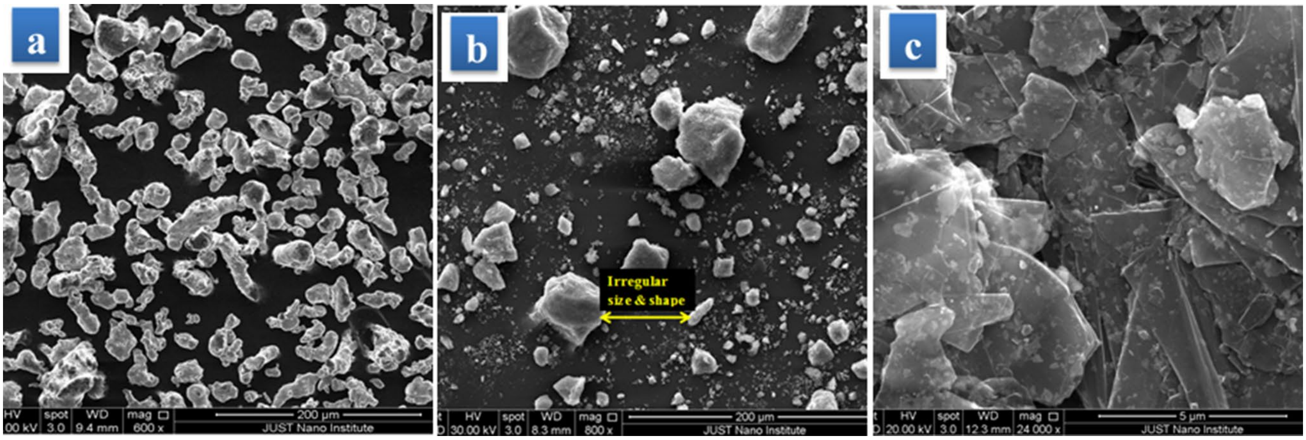

Fig. 2 SEM micrograph of **a** elongated sub-angular aluminum matrix, **b** irregular shapes and sizes of carbonized eggshells and **c** flake graphite

Fig. 3 Compaction process using universal testing machine

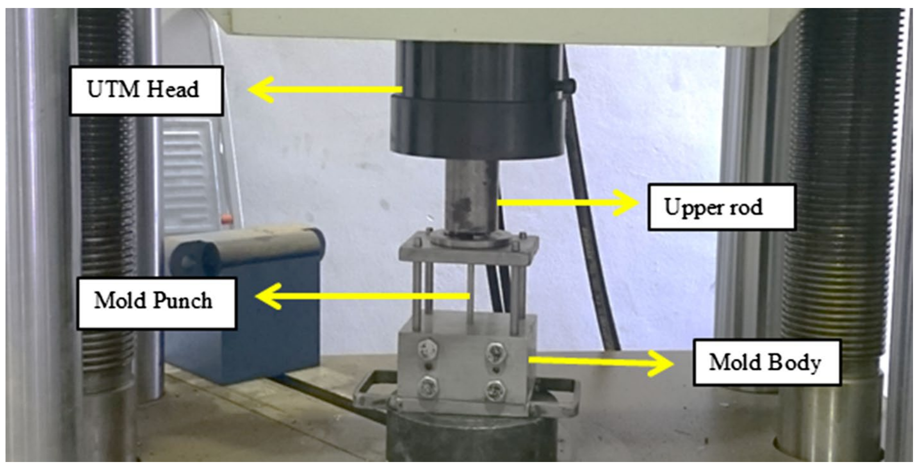

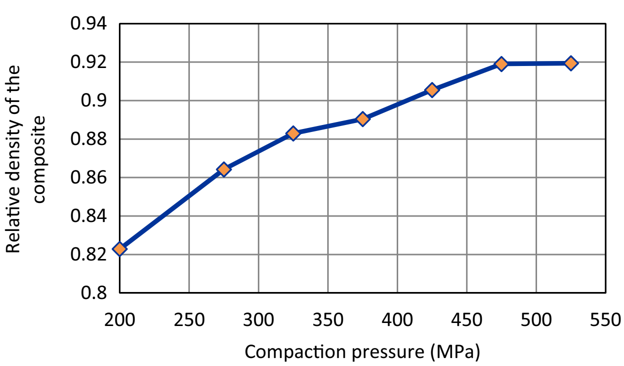

Fig. 4 Densification curves for Al matrix–6Es–3Gr composite

the applied pressure [29]. All produced samples were sintered at 630 °C for 2 h. Sintering was carried out in an electrical furnace. Sintering at high temperature can give enhanced physical and mechanical properties, as the powder compact goes through more densification with reduced porosity content and better particle bonding through progressive pores closure and neck formation between powder particles. The pores more likely become toward circular and smooth shape instead of having irregular and angular shape [30]. Zinc stearate lubricant, purchased from Sigma-Aldrich (USA), was coated on the internal surface of the mold cavity to facilitate sample removal after the compaction process. This step was performed as O'Donnell and Looney [31] suggested. The sample designation and reinforcement weight ratio are presented in Table 1.

2.3 Density and porosity calculations

It is essential to study the main factors of the produced hybrid metal matrix composites namely density and volume porosity percentage to illustrate the properties of composite materials. The theoretical density of the samples was calculated using the rule of mixtures as follows [32, 33]:

Table 1 Sample designation and reinforcement weight ratio

Sample No.	Sample designation	Es (wt%)	Gr (wt%)
1	Al matrix	0	0
2	Al matrix–1.5Gr	0	1.5
3	Al matrix–3Gr	0	3
4	Al matrix–4.5Gr	0	4.5
5	Al matrix–3Es–1.5Gr	3	1.5
6	Al matrix–3Es–3Gr	3	3
7	Al matrix–3Es–4.5Gr	3	4.5
8	Al matrix–6Es–1.5Gr	6	1.5
9	Al matrix–6Es–3Gr	6	3
10	Al matrix–6Es–4.5Gr	6	4.5
11	Al matrix–9Es–1.5Gr	9	1.5
12	Al matrix–9Es–3Gr	9	3
13	Al matrix–9Es–4.5Gr	9	4.5

$$\rho_{\text{Composite}} = \frac{100}{\frac{w1}{\rho 1} + \frac{w2}{\rho 2} + \frac{w3}{\rho 3}} \tag{1}$$

where ρ_1, ρ_2 and ρ_3 represent the density of the three material powders, while w_1, w_2 and w_3 represent the weight percentages of those powders.

In the present research, the volume porosity percentage of hybrid metal matrix composites has been examined based on the determination of the density of hybrid composites. Using Archimedes principle, experimental values of the density of the hybrid composites have been evaluated, and using the rule of mixtures, theoretical values of the density of the composites have been accomplished. Experimentally, the volume porosity percentage of the composite materials has been determined as follows [34]:

$$\text{Volume porosity}(\%) = 100 - \left(\frac{\text{sintered density}}{\text{theoretical density}} \right) \times 100 \tag{2}$$

2.4 Mechanical, tribological and microstructural characterizations

The compression test was performed by Quasar 100 universal testing machine at a crosshead speed of 2 mm/min. The aspect ratio of investigated samples ranged from 1.9 to 1.96. Reducing the barreling shape effect was done by coating the machine bench and crosshead with a thin layer of grease. Micro-Vickers hardness testing machine (model MHT1, Tokyo, Japan) was set at a load of 100 gf for a dwell time of 10 s. Seven readings were taken from each sample. The surface of the samples was polished by 0.3 µm diamond paste (alumina suspension, PRESI) to clarify the pyramid indentation, thereby showing more accurate results. The wear test was carried out according to ASTM G 99–95a [35] using a pin-on-disk apparatus (model TM 200, Gunt, Hamburg). The parameters of the test were set at a load of 25 N and a speed of 100 RPM. Al matrix, Al matrix–3Gr and Al matrix–6Es–3Gr composites were analyzed. Scanning electron microscope (Quanta™ 450 FEG SEM) supplied with energy-dispersive spectroscopy (EDS) was used to investigate reinforcement distribution, cracks, reinforcement–matrix interface and the type of wear mechanism.

3 Results and discussion

3.1 Density and porosity analysis

Table 2 shows the theoretical density, experimental density and volume porosity percentage of the produced composites. For easier interpretation, the volume porosity percentage in Table 2 is represented in Fig. 5. As shown in the figure, increasing Gr percentages caused the porosity to increase. Adding 4.5 wt% of Gr gave the highest amount of porosity regardless of the level of Es. Meanwhile, the addition of 1.5 wt% of Gr causes a slight increase in porosity volume percentage as compared to Al matrix.

3.2 The effect of graphite percentage and sliding time on wear Loss

Figure 6 shows the change in mass loss of the Al matrix–(X) Gr composites with sliding time at different weight fractions of graphite. Graphite content of 1.5 wt% and 3 wt% causes only a slight increase in wear loss as the graphite lubricant forms a thin layer that prevents metal to metal contact. This is similar to findings by previous researchers [21, 22, 36]. However, at 4.5 wt% graphite, a significant incremental increase in the mass loss is observed, due to the high amount of porosity similar behavior was reported by other researchers [37–39].

3.3 The effect of hybrid green reinforcement percentage and sliding time on wear loss

For all the examined composites, keeping the eggshell weight percentages constant and changing the graphite contents will result in an increase in the mass loss. As an example, Fig. 7 shows the variation of the mass loss with sliding time for composites having 3 wt% eggshell and different weight fractions of graphite (1.5, 3, 4.5). The increased mass loss with the increase in graphite percentages is due to the increase in porosity which is attributed to poor Al–Gr interface and clustering. On the other hand,

Table 2 Theoretical, experimental and relative density and porosity volume percentage of all produced samples

Sample No.	Composite type	Sintered density (g/cm^3)	Theoretical density (g/cm^3)	Porosity volume (%)
1	Al matrix	2.526	2.703	6.539
2	Al matrix–1.5Gr	2.496	2.692	7.270
3	Al matrix–3Gr	2.471	2.680	7.802
4	Al matrix–4.5Gr	2.437	2.669	8.686
5	Al matrix–3Es–1.5Gr	2.486	2.685	7.420
6	Al matrix–3Es–3Gr	2.457	2.674	8.108
7	Al matrix–3Es–4.5Gr	2.443	2.662	8.257
8	Al matrix–6Es–1.5Gr	2.485	2.679	7.229
9	Al matrix–6Es–3Gr	2.441	2.667	8.481
10	Al matrix–6Es–4.5Gr	2.425	2.656	8.720
11	Al matrix–9Es–1.5Gr	2.482	2.672	7.133
12	Al matrix–9Es–3Gr	2.463	2.661	7.445
13	Al matrix–9Es–4.5Gr	2.435	2.650	8.114

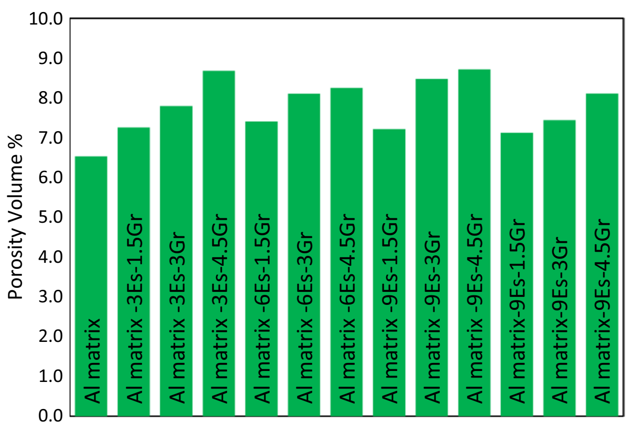

Fig. 5 Porosity volume percentage of all fabricated composites

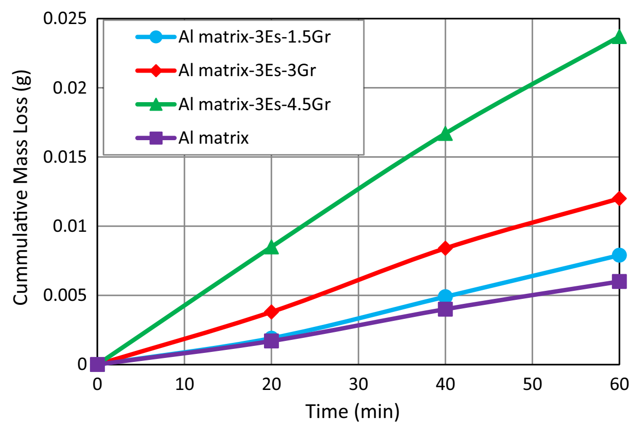

Fig. 7 Variation of cumulative mass loss of Al matrix–3Es–(X)Gr composites with varying graphite percentage and sliding time

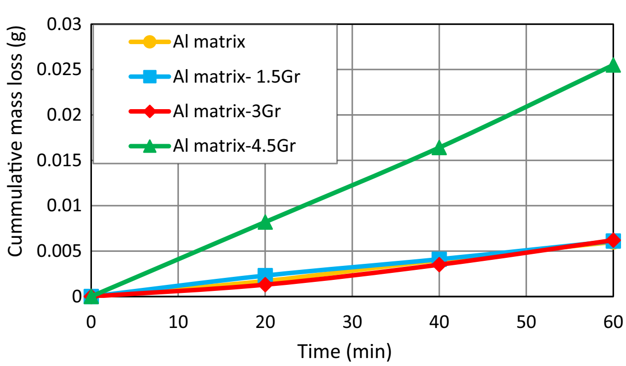

Fig. 6 Variation of cumulative mass loss of Al matrix–(X)Gr composites with sliding time at different graphite percentages

constant slope indicates that the wear loss is approximately uniform throughout the test.

3.4 The effect of porosity percentage on wear loss

Figure 8 shows the cumulative mass loss (after 60 min) versus porosity volume percentages for the examined Al matrix–(X)Gr composites at different graphite weight percentages. The figure showed that the mass loss increased with the increase in graphite content and thus porosity percentage. This behavior was also observed by Sinha and Farhat [34].

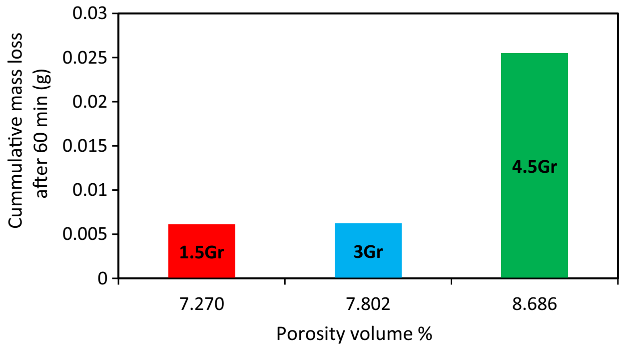

Fig. 8 Cumulative mass loss after 60 min versus porosity vol% for Al matrix–(X)Gr composite

3.5 The effect of graphite percentage on micro-Vickers hardness

Figure 9 displays the effect of graphite addition on the hardness of Al matrix. The addition of 1.5 Gr wt% increased the hardness from 30.3 to 31.9, i.e., which is about 5%. This improvement may be attributed to the presence of magnesium carbonate (magnesite, $MgCO_3$) hard phase. The presence of this hard phase reduced the amount of plastic deformation during the penetration of the indenter; therefore, the hardness will be increased. These results are consistent with the results presented by Hanna et al. [40]. However, the use of higher graphite content caused the hardness to decrease, where the hardness improvement decreased from 5% to 1.6% and 1.9% at 3 and 4.5 wt% Gr, respectively. The reduction in the hardness value can be attributed to the softness nature of graphite [19] and the increase in the porosity percentage with increasing graphite content. Similar results were presented in [15].

3.6 The effect of hybrid green reinforcement percentage on micro-Vickers hardness

Figure 10 depicts the effect of hybrid green reinforcement on the hardness of Al matrix. It can be seen from the figure that increasing graphite percentages, regardless of the constant amount of Es, always lead to a decrease in the hardness except the sample that contains 6 Es wt% and 3 Gr wt%. This increase may be reasoned to the penetration of the indenter directly in presented hard phases in the sample. All composites that contain 3 wt% Es with different percentages of Gr are characterized by higher values compared to Al matrix. However, Al matrix–9Es–4.5Gr composite has the lowest HV numbers. This is due to the presence of the highest amount of reinforcement which accompanied by a high amount of porosity. Hardness behavior in the present composites gives an initial indication of the mass loss behavior. In other words, the samples that have high hardness have lower mass loss according to the Archard equation, Eq. 3 [41]. Many researchers clarify the inverse relationship between wear rate and hardness [42, 43].

$$Q = \left(\frac{W}{H}\right) \tag{3}$$

Q represents the wear rate. K, W and H represent the wear coefficient constant, the normal load and the hardness, respectively.

3.7 The effect of graphite percentage on compressive strength

Figure 11 illustrates the relationship between graphite percentages and compressive strength. The addition of flake graphite up to 1.5 wt% increased compressive strength by 23%, and similar result is obtained by Swamy et al. [44].

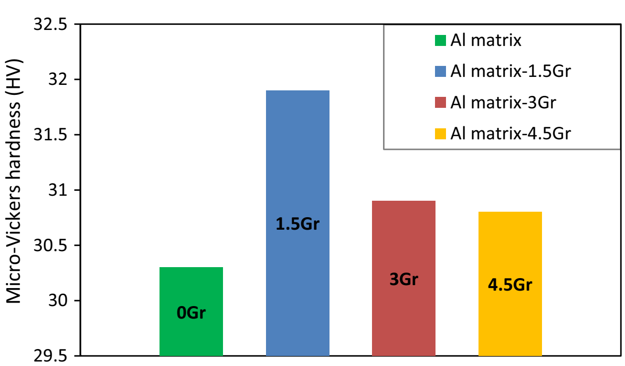

Fig. 9 Hardness values against graphite wt% in Al matrix–(X)Gr composites

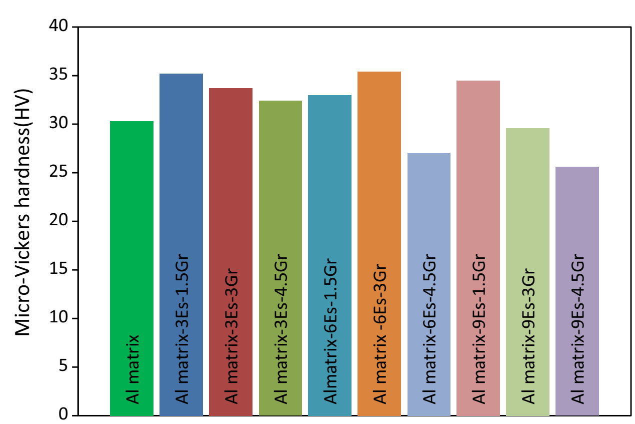

Fig. 10 Hardness values against hybrid green content in Al matrix–(X)Es–(X)Gr composites

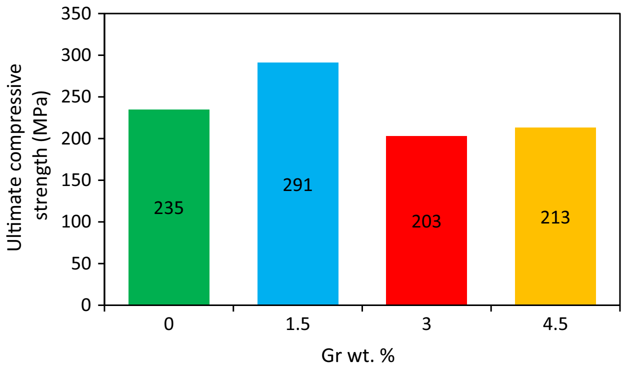

Fig. 11 Graph of compressive strength of Al matrix–(X)Gr composite

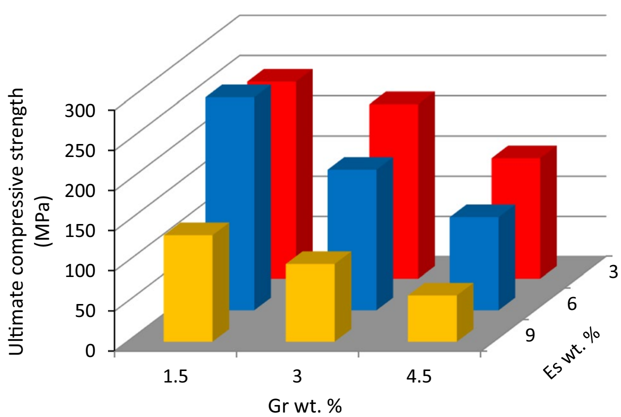

Fig. 12 Graph of compressive strength of Al matrix–(X)Es–(X)Gr composite

Beyond 1.5 wt% Gr, the compressive strength decreased again. At 1.5 Gr wt%, the amount of porosity was low; thus, the graphite, in turn, acts as a dislocation barrier improving compressive strength. Further, forming $MgCO_3$ may help in compressive strength improvement [40]. Meanwhile, at 3 and 4.5 Gr wt%, the compressive strength decreased due to the presence of the high amount of porosity that causes a reduction in the cross-sectional area, resulting in high stress concentration. Furthermore, the porosity at matrix–particle interface reduces the amount of transmitted load to reinforcement particles, where transmission load from the matrix to reinforcement largely depends on interfacial bonding; therefore, the strength of overall composite will be decreased [45].

3.8 The effect of hybrid green reinforcement percentages on compressive strength

According to Fig. 12, generally, it can be observed that the best hybrid green reinforcement is the combination of 3 Es wt% with different Gr wt%. In contrast, the worst hybrid green reinforcement is a combination of 9 wt% Es with different Gr wt%. This refers to the high amount of reinforcement which is accompanied by porosity which causes the lower strength of the material as discussed earlier [46]. The combination of 6 wt% Es with different percentages of Gr takes values between 3 and 9 wt% Es. It can be said that the wear, compressive strength and hardness results are in good agreement.

3.9 Microstructure and surface morphology

Although the graphite is a solid lubricant, its usefulness depends on several factors such as porosity, surface finish and the interface between matrix and particles [37]. In any case, a comparison of composite structures containing different graphite wt% (0, 1.5 and 3) was made. The micrograph of the SEM of Al matrix is displayed in Fig. 13. It is noticed from the figure that there is a homogenous distribution of sintering aids (Mg and Sn) in the Al matrix. Further, the shape of tin particles was changed during the sintering process which means these particles were melting during the process. However, Fig. 15 (at 0 wt% of Gr) presents a lower amount of porosity when compared to Figs. 14 and 15 (at 1.5 and 4.5 wt% of Gr, respectively). In the case of Al matrix, it was observed that even the porosity that existed was shallow as shown in Fig. 13. Yellow large squares in Fig. 15 display higher magnification for reds mall squares.

It is worthwhile to highlight here that the amount of porosity increased with increasing percentages of graphite flakes. This is clear in Figs. 14 and 15. As shown in Figs. 14, 15 and 16, the regions that include graphite flakes contain pores due to the poor matrix–particle interface. These pores cause crack initiation and therefore interconnected porosity. Figure 14 shows the agglomeration of graphite flakes which causes defects in the composites due to the presence of pores. These agglomerates form weak points in the composite leading to undesirable properties. A similar result was concluded by Ahmad et al. [47]. Figure 15a clearly depicts poor wettability between flake graphite and aluminum matrix, and it shows higher interconnected porosity compared to Fig. 14 that contains a lower percentage of graphite (1.5 Gr wt%). Furthermore, Fig. 15b shows the interconnected porosity in another location of the same sample which contains 4.5 Gr wt%. Higher focusing on poor matrix–particle interface is shown in Fig. 16.

For ease and convenience, the sample containing 6 wt% of eggshells and 3 wt% of graphite (Al matrix–6Es–3Gr) was taken to reflect the rest of the samples containing hybrid green reinforcement of Es and Gr. Figure 17 shows Es, Gr, Sn and Mg particles. Some clusters of these fine particles are observed. Also, we can observe that Es particles have irregular shapes and sizes due to shear force from blender

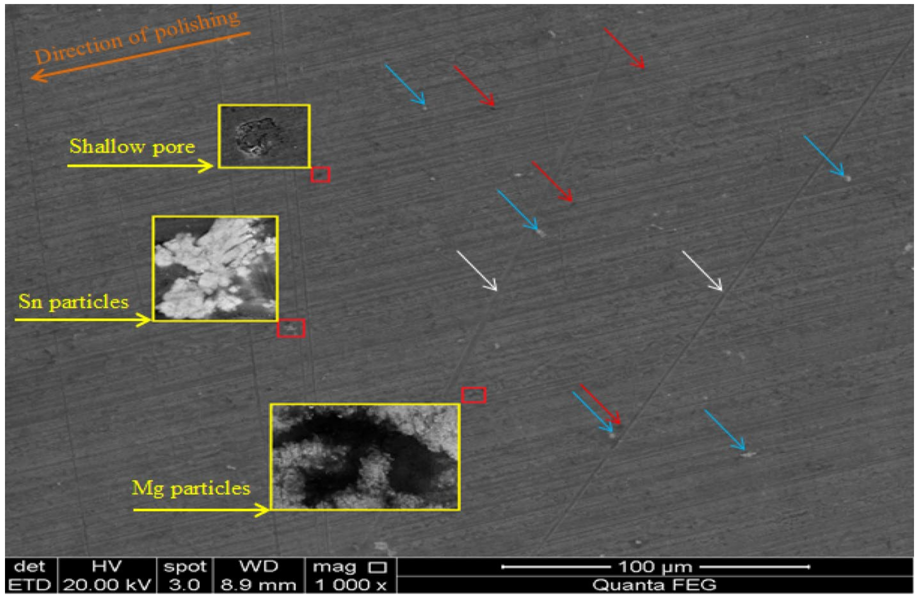

Fig. 13 SEM micrograph of Al matrix surface displaying low amount of porosity. Blue arrows (bright phase) indicate Sn particles, red arrows (dark phase) indicate Mg particles and white arrows indicate scratches (color figure online)

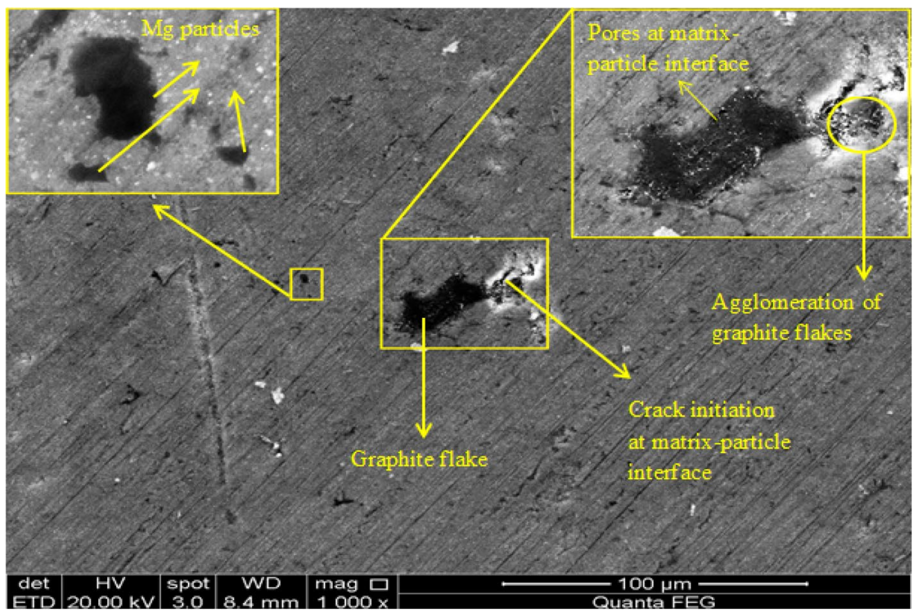

Fig. 14 SEM micrographs of polished surface of Al matrix–1.5Gr showing agglomeration, deep pores at matrix–particle interface and higher amount of porosity

blades as mentioned before. However, the porosity at the matrix–graphite interface is observed. Also, the porosity at the Es cluster has appeared.

3.10 Analysis of worn-out surfaces using SEM and EDX

The morphology of the worn-out surface is crucial for determining the wear mechanism in the composites. For the base monolithic matrix alloy, SEM micrographs shown in Fig. 18a conclude that different wear mechanisms were involved, i.e., adhesive and delaminated wear. Abrasive wear mechanism is characterized by the grooves on the surface. Platelike debris is clues for adhesive wear occurrence, and shallow cavities on the surface are result of delamination wear. Figure 18b presents the acquired EDS spectrum for the worn-out surface, which consists of peaks for oxygen, chromium and iron. The oxygen peak is a sign for the oxide formation at the interfacial sample surface and steel disk, where friction can cause an increase in the temperature and thus promote formation of oxide. The presence of iron and chromium peaks can be attributed to the transfer of steel disk asperities to the worn-out surface.

Composites containing 1.5 wt% graphite have similar features of that observed in the aluminum matrix. Moreover, fragmentation of graphite flakes laid on the delaminated regions is shown in Fig. 19. SEM images show the

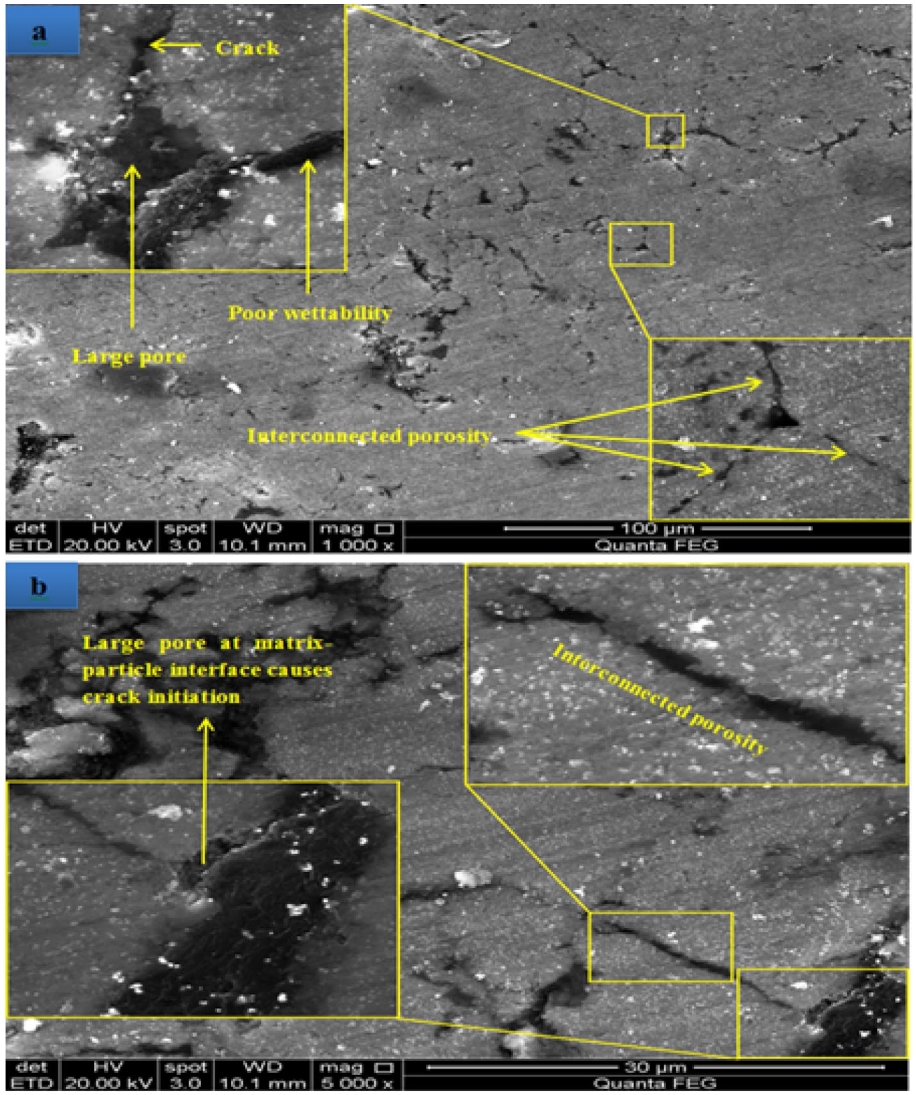

Fig. 15 SEM micrographs of a polished surface of Al matrix–4.5Gr of 2 locations. The first location **a** shows poor wettability, large pores, cracks and interconnected porosity at matrix–particle interface. The second location **b** also shows interconnected porosity at matrix–particle interface. Note the amount of porosity is presented in Al matrix–4.5Gr

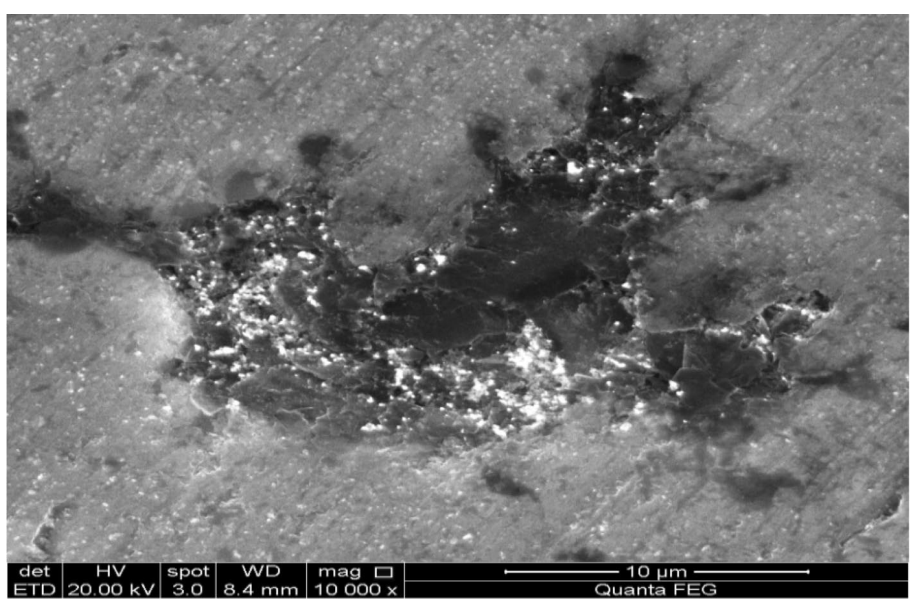

Fig. 16 SEM micrograph of Al matrix–1.5Gr composite showing particle matrix interface

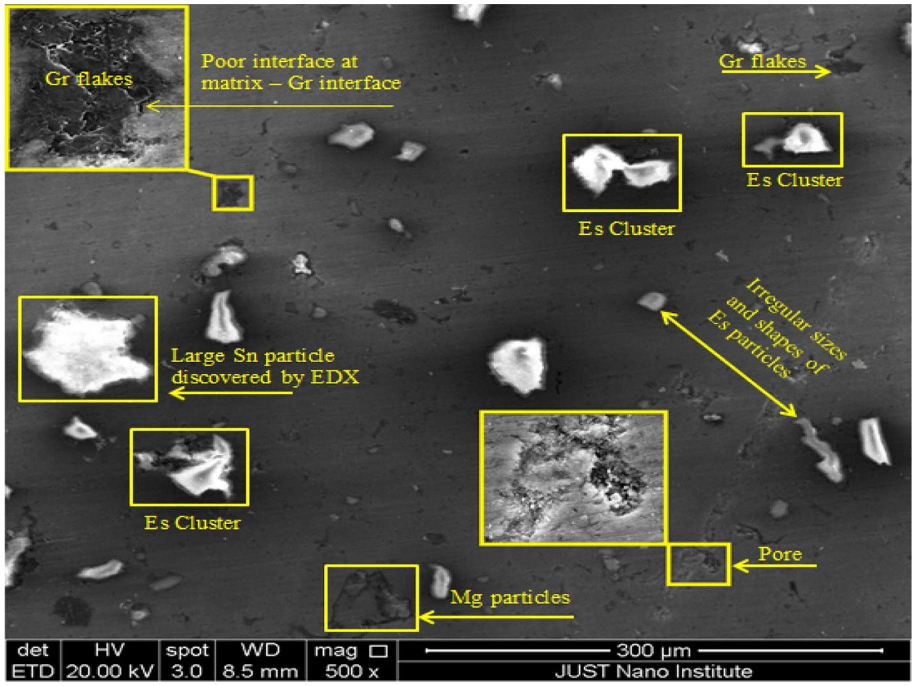

Fig. 17 SEM micrograph of Al matrix–6Es–3Gr composite showing Es clusters accompanied with porosity. Also, Gr, Sn and Mg are appeared

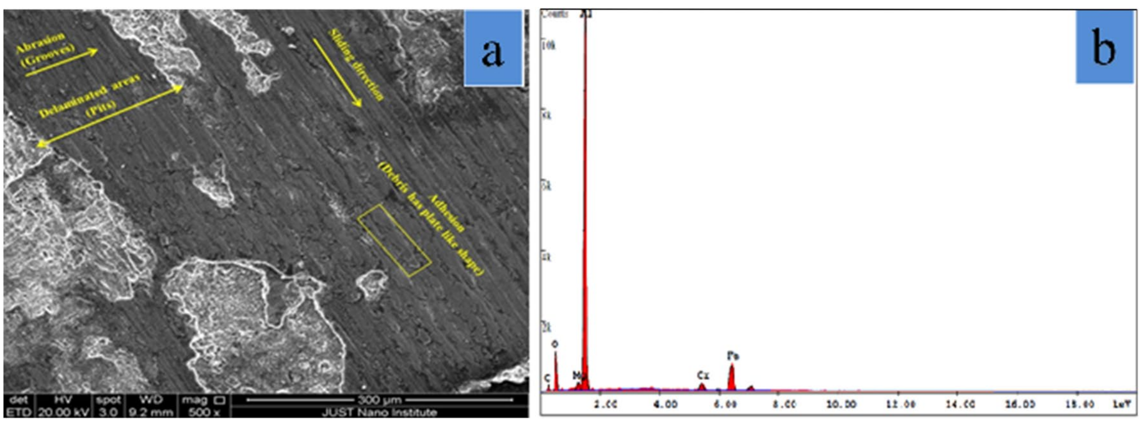

Fig. 18 **a** SEM micrograph of worn-out surfaces of Al matrix alloy showing three types of wear: abrasion, adhesion and delamination wear, **b** EDX analysis of worn-out surface of Al matrix alloy

occurrence of alteration of the wear mechanisms of the composites containing 4.5 wt% graphite, where the adhesive wear becomes more dominant as shown in Fig. 20. In addition, some pores appeared on the surface as a result of the graphite that is pulled out of the surface. The magnified image of one of these pores shows fragmentations of graphite flakes.

4 Conclusions

The goal of this research is to examine the effect of incorporating both graphite and eggshell as reinforcement particles on mechanical (hardness, compressive strength) and tribological properties of the powder aluminum matrix. The main points that can be drawn as follows:

1. An enhancement of the compressive strength and hardness of the matrix alloy was attained by adding 1.5 wt% graphite as a result of the formation of $MgCO_3$. However, the use of 3 wt% and 4.5 wt% of graphite decrease both the compressive strength and hardness of the composite as a result of the increase in porosity percentage and thus reduction in the transmitted load to the matrix.
2. Adding graphite to the aluminum matrix composite containing eggshell has a positive impact on the tribological properties of the composite to a certain limit (1.5 wt%).

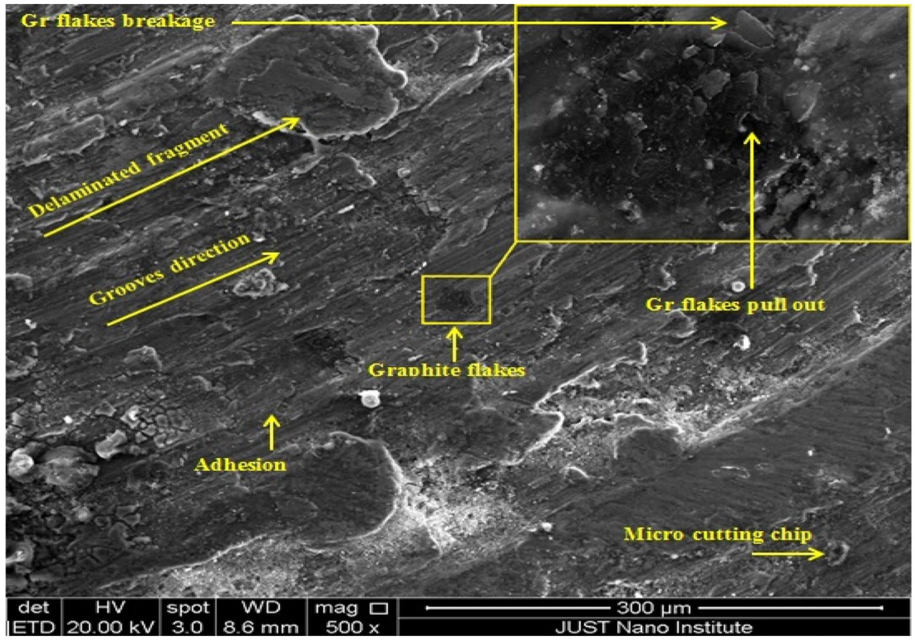

Fig. 19 SEM micrograph of worn-out surfaces of Al matrix–1.5Gr composite showing the three types of wear and agglomeration, pullout and breakage of graphite flakes

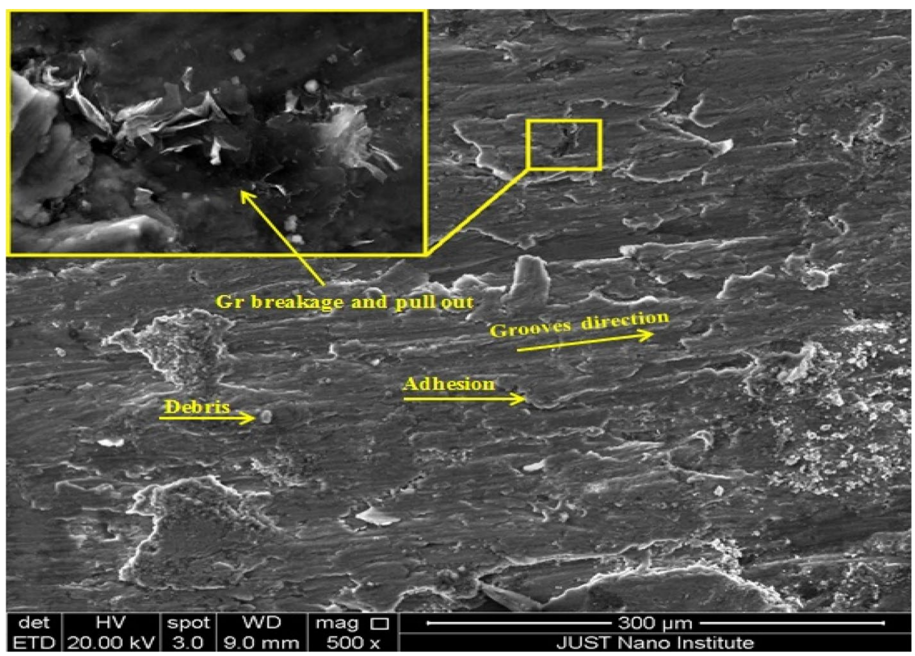

Fig. 20 SEM micrograph of worn-out surfaces of Al matrix–4.5Gr composite showing the same three types of wear, agglomeration, pullout and breakage of graphite flakes

However, the additional increase in graphite content has an adverse effect.

3. Hybrid composites with 3 wt% eggshell show the best compressive strength and hardness, whereas hybrid composite with 9 wt% eggshell has the lowest compressive strength and hardness.
4. The mass loss of the hybrid composite increases with the increase in the graphite weight percentages, regardless of the eggshell weight percentages. This was attributed to the increase in clustering and porosity content with the increase in graphite content and the poor interface of aluminum graphite interface.
5. Composites with higher porosity contents have lower hardness and compressive strength, but higher wear rate as compared with composites having lower porosity contents.
6. The combination of SEM micrographs and EDX showed signs for four wear mechanisms: abrasive, adhesive, delaminated and oxidative wear in the examined composites.

Acknowledgements The authors are grateful for the Deanship of Scientific Research at Jordan University of Science and Technology (JUST) for the generous fund and support with Grant No. 256/2017.

References

1. Sabatini G, Ceschini L, Martini C et al (2010) Improving sliding and abrasive wear behaviour of cast A356 and wrought AA7075 aluminium alloys by plasma electrolytic oxidation. Mater Des 31:816–828
2. Abdizadeh H, Ashuri M, Moghadam P et al (2011) Improvement in physical and mechanical properties of aluminum/zircon composites fabricated by powder metallurgy method. Mater Des 32:4417–4423
3. Canakci A, Varol T (2014) Microstructure and properties of AA7075/Al–SiC composites fabricated using powder metallurgy and hot pressing. Powder Technol 268:72–79
4. Chaithanyasai A, Vakchore Pand Umasankar V (2014) The micro structural and mechanical property study of effects of egg shell particles on the aluminum 6061. Procedia Eng 97:961–967
5. Pournaderi S, Akhlaghi F (2017) Wear behaviour of Al6061–Al_2O_3 composites produced by in situ powder metallurgy (IPM). Powder Technol 313:184–190
6. Ekambaram M, Vetrivel M, Balaji D, Shahid Afrid A, Naveenkumar B, Raja Manikanta D et al (2018) Tribological characteristics of aluminium metal matrix with nano BN powder metallurgy composite. IOP Conf Ser Mater Sci Eng 390:012085
7. Almomani M, Hayajneh M, Draidi M (2015) Tribological investigation of zamak alloys reinforced with alumina (Al_2O_3) and fly ash. Part Sci Technol 34:317–323
8. Lakshmipathy J, Rajesh Kannan S, Manisekar K et al (2017) Effect of reinforcement and tribological behaviour of AA7068 hybrid composites manufactured through powder metallurgy techniques. Appl Mech Mater 867:19–28
9. Sharma S, Dwivedi S (2017) Effects of waste eggshells and SiC addition on specific strength and thermal expansion of hybrid green metal matrix composite. J Hazard Mater 333:1–9
10. Toro P, Quijada R, Yazdani-Pedram M et al (2007) Eggshell a new bio-filler for polypropylene composites. Mater Lett 61:4347–4350
11. Bootklad M, Kaewtatip K (2013) Biodegradation of thermoplastic starch/eggshell powder composites. Carbohydr Polym 97:315–320
12. Hassan T, Rangari V, Jeelani S (2014) Value-added biopolymer nanocomposites from waste eggshell-based $caco_3$ nanoparticles as fillers. ACS Sustain Chem Eng 2:706–717
13. Iyer K, Torkelson J (2014) Green composites of polypropylene and eggshell: effective biofiller size reduction and dispersion by single-step processing with solid-state shear pulverization. Compos Sci Technol 102:152–160
14. Boronat T, Fombuena V, Garcia-Sanoguera D et al (2015) Development of a biocomposite based on green polyethylene biopolymer and eggshell. Mater Des 68:177–185
15. El-Sayed Seleman M, Ahmed M, Ataya S (2018) Microstructure and mechanical properties of hot extruded 6016 aluminum alloy/graphite composites. J Mater Sci Technol 34:1580–1591
16. Podgornik B, Kosec T, Kocijan A et al (2015) Tribological behaviour and lubrication performance of hexagonal boron nitride (h-BN) as a replacement for graphite in aluminium forming. Tribol Int 281:267–275
17. Arik H (2008) Effect of mechanical alloying process on mechanical properties of α-Si_3N_4 reinforced aluminum-based composite materials. Mater Des 29:1856–1861
18. Sarkar S, Sen S, Mishra S et al (2008) Studies on aluminum: fly-ash composite produced by impeller mixing. J Reinf Plast Compos 29:144–148
19. Hassan A, Tashtoush G, Al-Khalil J (2006) Effect of graphite and/or silicon carbide particles addition on the hardness and surface roughness of Al-4 wt% Mg alloy. J Compos Mater 41:453–465
20. Ravindran P, Manisekar K, Narayanasamy P et al (2012) Application of factorial techniques to study the wear of Al hybrid composites with graphite addition. Mater Des 39:42–54
21. Ravindran P, Manisekar K, Narayanasamy R et al (2013) Tribological behaviour of powder metallurgy-processed aluminium hybrid composites with the addition of graphite solid lubricant. Ceram Int 39:1169–1182
22. Iacob G, Ghica V, Buzatu M et al (2015) Studies on wear rate and micro-hardness of the Al/Al_2O_3/Gr hybrid composites produced via powder metallurgy. Compos B 69:603–611
23. Hassan S, Aigbodion V (2017) Effects of eggshell on the microstructures and properties of Al–Cu–Mg/eggshell particulate composites. J King Saud Univ Eng Sci 27:49–56
24. Dwivedi S, Sharma S, Mishra R (2016) Mechanical and metallurgical characterizations of AA2014/eggshells waste particulate metal matrix composite. Int J Precis Eng Manuf Green Technol 3:281–288
25. Razavi Hesabi Z, Hafizpour H, Simchi A (2017) An investigation on the compressibility of aluminum/nano-alumina composite powder prepared by blending and mechanical milling. Mater Sci Eng A 454:89–98
26. Xie G, Ohashi O, Sato T et al (2004) Effect of Mg on the sintering of Al–Mg alloy powders by pulse electric-current sintering process. Mater Trans JIM 45:904–909
27. MacAskill I, Hexemer R, Donaldson I et al (2010) Effects of magnesium, tin and nitrogen on the sintering response of aluminum powder. J Mater Process Technol 210:2252–2260
28. Jamal N, Yusof F, Nor Y, Othman M, Khalid K, Zakaria M (2018) The role of tin and magnesium in assisting liquid phase sintering of aluminum (Al). IOP Conf Ser Mater Sci Eng 290:012008
29. Ghita C, Popescu I (2012) Experimental research and compaction behaviour modelling of aluminium based composites reinforced with silicon carbide particles. Comput Mater Sci 64:136–140
30. Almomani M, Shatnawi A, Alrashdan M (2015) Effect of sintering time on the density, porosity content and microstructure of copper: 1 wt% silicon carbide composites. Adv Mater Res 1064:32–37
31. O'Donnell G, Looney L (2001) Production of aluminium matrix composite components using conventional PM technology. Mater Sci Eng A 303:292–301
32. Liu J, Khan U, Coleman J et al (2016) Graphene oxide and graphene nanosheet reinforced aluminium matrix composites: powder synthesis and prepared composite characteristics. Mater Des 94:87–94
33. Kok M (2005) Production and mechanical properties of Al_2O_3 particle-reinforced 2024 aluminium alloy composites. J Mater Process Technol 161:381–387
34. Sinha A, Farhat Z (2015) Effect of surface porosity on tribological properties of sintered pure al and Al 6061. Mater Sci Appl 06:549–566
35. ASTM G99-95a (2000) Standard test method for wear testing with a pin-on-disk apparatus
36. Akhlaghi F, Zare-Bidaki A (2009) Influence of graphite content on the dry sliding and oil impregnated sliding wear behavior of Al 2024–graphite composites produced by in situ powder metallurgy method. Wear 266:37–45
37. Jha A, Prasad S, Upadhyaya G (1989) Dry sliding wear of sintered 6061 aluminium alloy: graphite particle composites. Tribol Int 22:321–327

38. Mahdavi S, Akhlaghi F (2011) Effect of the graphite content on the tribological behavior of Al/Gr and Al/30SiC/Gr composites processed by in situ powder metallurgy (IPM) method. Tribol Lett 44:1–12
39. Sahin S, Yüksel N, Hülya D, Ýrýzalp S (2013) Wear behavior of Al/SiC/graphite and Al/Feb/graphite hybrid composites. Mater Tehnol 4:639–646
40. Hanna W, Gharib F, Marhoon I (2011) Characterization of ceramic filled polymer matrix composite used for biomedical applications. J Miner Mater Charact Eng 10:1167–1178
41. Nemati N, Khosroshahi R, Emamy M et al (2011) Investigation of microstructure, hardness and wear properties of Al–4.5wt.% Cu–TiC nanocomposites produced by mechanical milling. Mater Des 32:3718–3729
42. Ahlatci H, Koçer T, Candan E et al (2006) Wear behaviour of Al/(Al_2O_3p + SiCp) hybrid composites. Tribol Lett 39:213–220
43. Mondal D, Das S (2006) High stress abrasive wear behaviour of aluminium hard particle composites: effect of experimental parameters, particle size and volume fraction. Tribol Lett 39:470–478
44. Swamy A, Ramesha A, Kumar G et al (2011) Effect of particulate reinforcements on the mechanical properties of Al6061-WC and Al6061-Gr MMCs. J Miner Mater Charact Eng 10:1141–1152
45. Rashad M, Pan F, Tang A et al (2014) Effect of graphene nanoplatelets addition on mechanical properties of pure aluminum using a semi-powder method. Prog Nat Sci Mater Int 24:101–108
46. Gopal P, Soorya Prakash K, Nagaraja S et al (2017) Effect of weight fraction and particle size of CRT glass on the tribological behaviour of Mg–CRT–BN hybrid composites. Tribol Lett 116:338–350
47. Ahmad F, Jaafar M, Palaniandy S et al (2008) Effect of particle shape of silica mineral on the properties of epoxy composites. Compos Sci Technol 68:346–353